Current Biology 19, 369–380, March 10, 2009 ©2009 Elsevier Ltd All rights reserved DOI 10.1016/j.cub.2009.01.064

Article

Regulation of APC/C Activity in Oocytes by a Bub1-Dependent Spindle Assembly Checkpoint

Barry E. McGuinness,[1,7] Martin Anger,[1,2,7,8] Anna Kouznetsova,[3] Ana M. Gil-Bernabé,[4,9] Wolfgang Helmhart,[1] Nobuaki R. Kudo,[4,10] Annelie Wuensche,[5] Stephen Taylor,[6] Christer Hoog,[3] Bela Novak,[2] and Kim Nasmyth[1,*]

[1]Department of Biochemistry
[2]Oxford Centre for Integrative Systems Biology
University of Oxford
South Parks Road
Oxford, OX1 3QU
United Kingdom
[3]Department of Cell and Molecular Biology
Karolinska Institutet
S-171 77 Stockholm
Sweden
[4]Research Institute of Molecular Pathology
Dr. Bohr-Gasse 7
A-1030 Vienna
Austria
[5]EMBL Heidelberg
Meyerhofstraße 1
69117 Heidelberg
Germany
[6]Faculty of Life Sciences
Michael Smith Building
Oxford Road
Manchester M13 9PT
United Kingdom

Summary

Background: Missegregation of chromosomes during meiosis in human females causes aneuploidy, including trisomy 21, and is thought also to be the major cause of age-related infertility [1]. Most errors are thought to occur at the first meiotic division. The high frequency of errors raises questions as to whether the surveillance mechanism known as the spindle assembly checkpoint (SAC) that controls the anaphase-promoting complex or cyclosome (APC/C) operates effectively in oocytes. Experimental approaches hitherto used to inactivate the SAC in oocytes suffer from a number of drawbacks.
Results: Bub1 protein was depleted specifically in oocytes with a Zp3-Cre transgene to delete exons 7 and 8 from a floxed *BUB1*^{F} allele. Loss of Bub1 greatly accelerates resolution of chiasmata and extrusion of polar bodies. It also causes defective biorientation of bivalents, massive chromosome missegregation at meiosis I, and precocious loss of cohesion between sister centromeres. By using a quantitative assay for APC/C-mediated securin destruction, we show that the APC/C is activated in an exponential fashion, with activity peaking 12–13 hr after GVBD, and that this process is advanced by 5 hr in oocytes lacking Bub1. Importantly, premature chiasmata resolution does not occur in Bub1-deficient oocytes also lacking either the APC/C's Apc2 subunit or separase. Finally, we show that Bub1's kinase domain is not required to delay APC/C activation.
Conclusions: We conclude that far from being absent or ineffective, the SAC largely determines the timing of APC/C and hence separase activation in oocytes, delaying it for about 5 hr.

Introduction

Chromosome segregation in eukaryotic cells depends on attachment of sister kinetochores to microtubules emanating from opposite poles of the cell, a process known as amphitelic attachment or biorientation [2]. This is achieved at least partly because of a system that corrects errors. Connections between kinetochores and microtubules are selectively stabilized, or rather become refractory to the disrupting effect of the Aurora B kinase, by tension created when bioriented sister chromatids [3] are pulled in opposite directions while being held together by the cohesin complex [4]. Disjunction of sister chromatids at the onset of anaphase is eventually triggered by cleavage of cohesin's kleisin subunit at the hands of a highly regulated protease called separase [5, 6], which is kept inactive for most of the cell cycle through the binding of an inhibitory chaperone called securin and phosphorylation by cyclin B/Cdk1 kinase [7]. Separase is activated only through destruction of securin and cyclin B at the hands of an ubiquitin protein ligase called the anaphase-promoting complex or cyclosome (APC/C) when all chromosomes have bioriented [8].

Because it triggers the removal from centromeres of the Aurora B kinase [9] as well as the loss of sister-chromatid cohesion, the APC/C must not be activated until chromosome biorientation has been completed. The regulatory mechanism responsible for delaying anaphase in this manner, known as the spindle assembly checkpoint (SAC) [10], requires, among others, the Mad1, Mad2, Bub1, and BubR1 proteins. With the help of Bub1, Mad1 binds to unattached, mono-oriented, or syntelically attached kinetochores and catalyzes sequestration of the APC/C's Cdc20 activator protein by a protein called Mad2. The Cdc20/Mad2 complex, together with yet another SAC protein called BubR1, binds to the APC/C and blocks its ability to ubiquitinylate either securin or cyclin B. Production of inhibitory Cdc20/Mad2/BubR1 complexes only ceases when all chromosomes have bioriented, which triggers the ubiquitinylation and subsequent destruction of securin and cyclin B by the APC/C, which in turn activates separase and triggers sister-chromatid disjunction. In the cells of some organisms, such as yeast [11] and flies [12], the SAC is not essential for mitosis, though it greatly reduces rare missegregation events. Loss of the SAC in mammalian cells, on the other hand, causes premature sister-chromatid disjunction

*Correspondence: kim.nasmyth@bioch.ox.ac.uk
[7]These authors contributed equally to this work
[8]Present address: Institute of Animal Physiology and Genetics, AS CR, v.v.i., Rumburska 89, 277 21 Libechov, Czech Republic and Veterinary Research Institute, Hudcova 70, 621 00 Brno, Czech Republic
[9]Present address: Radiation Oncology and Biology, The Radiobiology Research Institute, Churchill Hospital, University of Oxford, Oxford OX3 7LJ, United Kingdom
[10]Present address: Institute of Reproductive and Developmental Biology (IRDB), Imperial College London, Hammersmith Hospital, Du Cane Road, London W12 0NN, United Kingdom

and as a consequence massive chromosome missegration and lethality [13, 14]. Presumably because of the SAC, a single misaligned chromosome delays the onset of anaphase in tissue-culture cells [15].

During the first meiotic division, biorientation of sister kinetochores is explicitly blocked and the tension necessary to ensure that kinetochores attach stably to microtubules is instead created by traction toward opposite poles of maternal and paternal kinetochores, whose disjunction is prevented by the chiasmata holding bivalent (tetrad) chromosomes together [16]. The first meiotic division is eventually triggered by destruction of sister-chromatid cohesion by separase along chromosome arms but not at centromeres. This resolves chiasmata, splitting the bivalent into two meiosis II (dyad) chromosomes, each containing a parental and a recombinant chromatid.

A suggestion that the SAC might be missing in vertebrate oocytes and that this could explain the high incidence of human aneuploidy comes from studies of XO mice, which carry only a single X chromosome but are phenotypically female. Despite not having a homologous X chromosome available for recombination, such females are fertile, albeit at a reduced level. In one-third of oocytes, sister chromatids disjoin precociously at anaphase I, producing eggs with individual X chromatids, but in the remaining two-thirds of oocytes, univalent X chromosomes segregate, without any major delay in the onset of anaphase, either to the egg or to the first polar body [17, 18]. If the SAC were effective in oocytes, it should surely detect mono-oriented univalent X chromosomes and block the first meiotic division, so the argument goes.

The notion that the SAC is ineffective in oocytes has been challenged by the finding that inhibitors such as nocodazole, which interfere with microtubule dynamics, clearly block polar body extrusion (PBE) [19, 20] and the onset of securin proteolysis [21–23]. Depletion of Mad2 through injection of morpholino antisense oligonucleotides alleviates, albeit only partially, the inhibition of securin destruction and permits a minor fraction of oocytes to undergo polar body extrusion (PBE) in the presence of nocodazole. It also induces modest chromosome missegregation at meiosis I in untreated oocytes, possibly by advancing the onset of securin destruction by about 60 min [21]. Meanwhile, injection into GV mouse oocytes of mRNAs that overexpress an N-terminal fragment of Bub1 (Bub1 dn, aa1–331), which binds to kinetochores and is thought to block activity of the endogenous protein, advances PBE by 3 hr [24]. However, the experimental approaches hitherto used to address the role of the SAC in oocytes suffer from a number of drawbacks. These include the likelihood of incomplete knockdown RNA interference, the certainty that at least half the Mad2 protein persists in the *Mad2*$^{+/-}$ oocytes [25], and the possibility that overexpressed Bub1 dn [24] and Mad2 dn [20] have unknown or unforeseen effects. To overcome these limitations, we created mice in which the *BUB1* gene is deleted specifically in oocytes.

Results

Deletion of *BUB1* in Oocytes Causes Sterility and Advances Polar Body Extrusion

To inactive Bub1 in oocytes, female mice with exons 7 and 8 of the *BUB1* gene flanked with *LoxP* sites (*BUB1*^{F}) [14] were crossed to males that express Cre recombinase under the control of the *Zona pellucida 3* promoter (*Zp3-Cre*) [26], which is expressed exclusively during the early stages of growing oocytes [27]. Genotyping of offspring from crosses of *BUB1*$^{F/+}$ *Zp3-Cre* females to wild-type males showed that 64 out of 64 *BUB1*^{F} alleles were converted to *bub1*$^{\Delta}$ in the female germline. *BUB1*$^{F/+}$*Zp3-Cre* and *BUB1*$^{F/F}$ females are fertile. In contrast, not a single pregnancy was observed after 10 weeks in any one of six *BUB1*$^{F/F}$ *Zp3-Cre* females crossed to wild-type males. The ovaries of *BUB1*$^{F/F}$ *Zp3-Cre* females contained normal numbers of germinal vesicle (GV)-stage oocytes surrounded by cumulus cells (40–60 oocytes per female; data not shown).

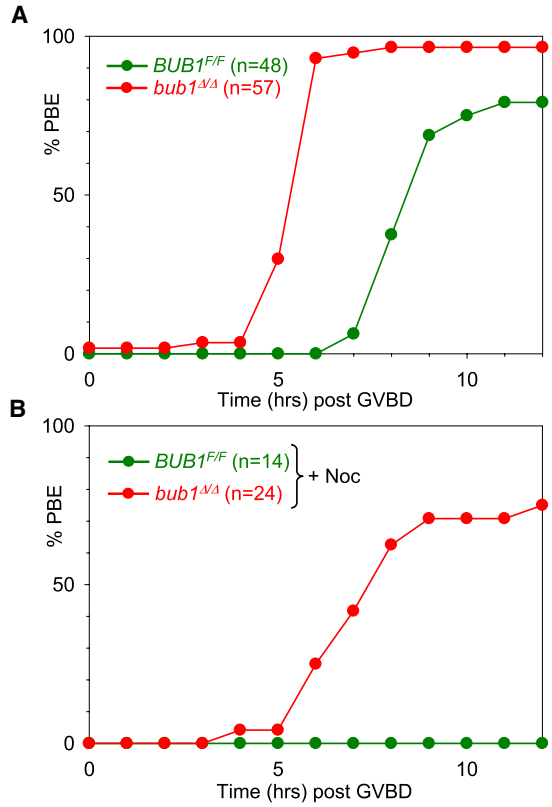

Figure 1. PBE Timing Is Advanced in *bub1*$^{\Delta/\Delta}$ Oocytes

(A) Kinetics of polar body extrusion (PBE). *BUB1*$^{F/F}$ and *bub1*$^{\Delta/\Delta}$ oocytes were harvested in M2 medium containing IBMX, which inhibits GVBD. Oocytes were released into inhibitor-free M16 medium. 90 min after release, those oocytes that had completed GVBD were selected for further analysis. This was set as time = 0 hr. Oocytes were monitored every hour and scored for completion of PBE.

(B) *bub1*$^{\Delta/\Delta}$ oocytes can escape a nocodazole-induced arrest. Oocytes were harvested and cultured as in (A) except nocodazole was added to the M16 medium at 5 μM from time = 0 hr until the end of the experiment.

To investigate Bub1's function during oocyte maturation, fully grown GV-stage mouse oocytes were harvested in the presence of IBMX from *BUB1*$^{F/F}$ females and *BUB1*$^{F/F}$ *Zp3-Cre* females (*bub1*$^{\Delta/\Delta}$). The two sets of oocytes underwent germinal vesicle breakdown (GVBD) with similar kinetics and efficiency upon removal of IBMX (data not shown). In contrast, the interval between GVBD and PBE was reduced from 08:30 ± 01:12 (n = 48) to 05:23 ± 01:04 hr (n = 57) by Bub1 depletion (Figure 1A). The fraction of cells that extruded a second polar body when cultured for 24 hr was equally low in *BUB1*$^{F/F}$ and *bub1*$^{\Delta/\Delta}$ oocytes (data not shown), which is consistent with the previous finding that CSF arrest was unaffected by a putatively dominant-negative Bub1 protein [24]. Strikingly, 75% of *bub1*$^{\Delta/\Delta}$ oocytes (n = 24) extruded the first polar body 07:20 ± 01:42 hr after GVBD (n = 18) in the presence of 5 μM nocodazole, a treatment that completely blocks PBE in *BUB1*$^{F/F}$ oocytes (n = 14) (Figure 1B).

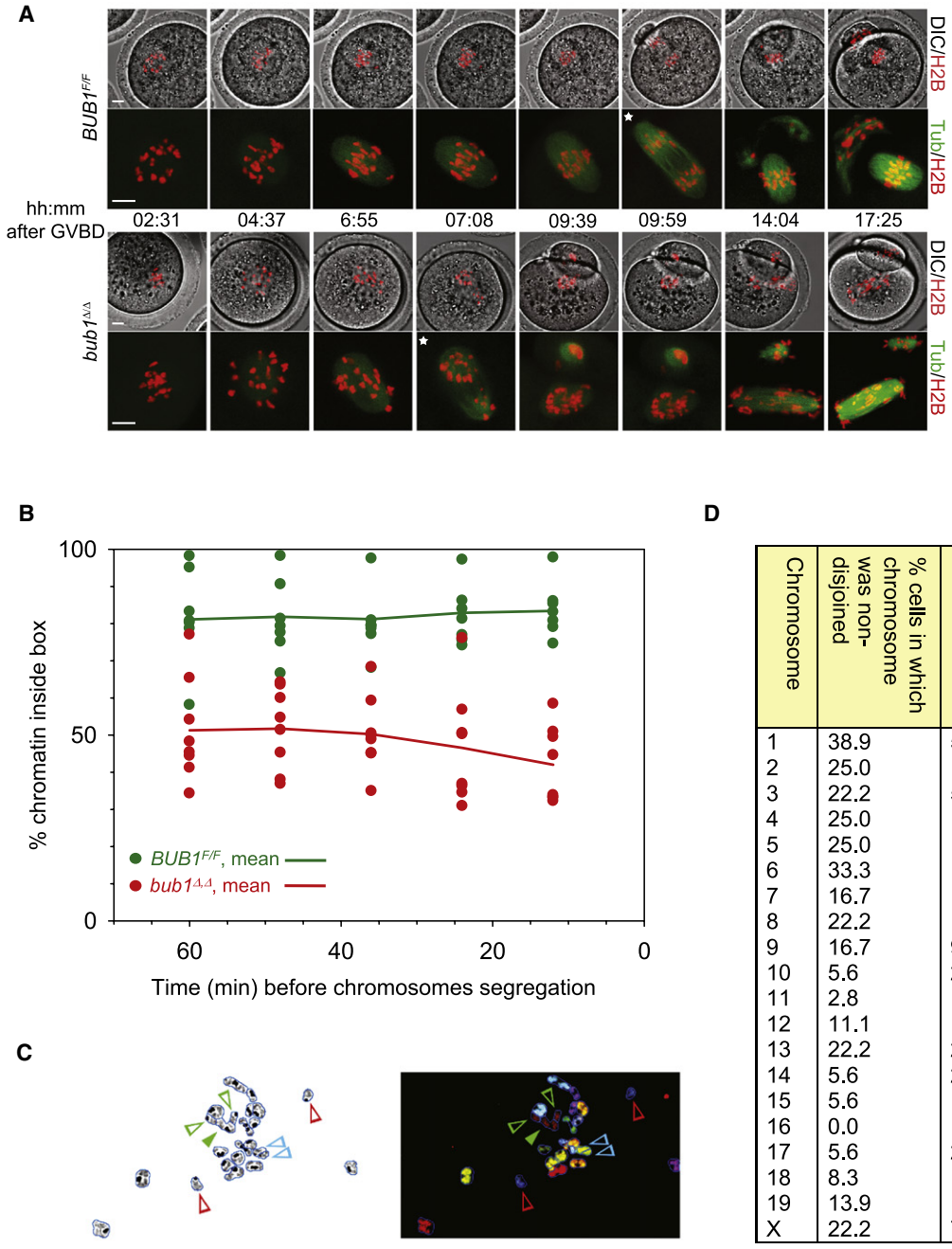

D

Chromosome	% cells in which chromosome was non-disjoined	% of separated chromatids as fraction of those observed
1	38.9	5.9
2	25.0	10.6
3	22.2	5.4
4	25.0	10.5
5	25.0	11.9
6	33.3	10.2
7	16.7	13.9
8	22.2	17.2
9	16.7	9.3
10	5.6	21.4
11	2.8	11.1
12	11.1	11.6
13	22.2	23.1
14	5.6	28.6
15	5.6	16.4
16	0.0	16.2
17	5.6	28.9
18	8.3	18.1
19	13.9	15.8
X	22.2	7.3

Figure 2. Chromosome Segregation in *bub1*$^{\Delta/\Delta}$ Oocytes Is Initiated prior to Congression to a Metaphase Plate

(A) Chromosome movements and microtubule spindle dynamics in *BUB1*$^{F/F}$ and *bub1*$^{\Delta/\Delta}$ oocytes expressing histone H2B-mCherry and β-Tubulin-EGFP were visualized by time-lapse confocal microscopy. Still images from a representative movie of each genotype are shown. The upper panels show DIC images merged with the H2B-mCherry channel pseudocolored in red. The lower panels show the H2B-mCherry and β-Tubulin-EGFP pseudocolored in red and green, respectively. The asterisks indicate the frame where chromosome segregation was first observed. Scale bars represent 10 μm.

(B) The extent of chromosome congression in movies similar to that shown in (A) was measured (see Figure S1) for the five frames prior to chromosome segregation and plotted against time. The oocytes were aligned relative to time of chromosome segregation. The solid lines show the mean values for each group of oocytes.

(C) *bub1*$^{\Delta/\Delta}$ MII oocytes were harvested 20 hr after hormonal stimulation. Chromosome spreads were prepared. An example of a chromosome spread stained with DAPI (left) and after hybridization with SKY probe (right) is shown. Chromosomes 7 (red arrows), 8 (blue arrows), and 11 (green arrows) with two single chromatids are indicated.

(D) Asymmetric distribution of chromosomes during meiosis I in *bub1*$^{\Delta/\Delta}$ oocytes. Frequency of segregation errors calculated for each chromosome. See text for details.

Chromosome Missegregation and Defective Congression in *bub1*$^{\Delta/\Delta}$ Oocytes

To investigate the effect of Bub1 ablation on chromosome segregation, we imaged oocytes that had been microinjected with mRNA for histone H2B-Cherry and β-Tubulin-EGFP (Figure 2A and Movie S2 available online). In *BUB1*$^{F/F}$ oocytes, chiasmata were only resolved and dyads segregated to the egg and first polar body after all bivalents had congressed,

forming a compact metaphase plate. Dyad chromosomes within the egg subsequently congressed to form metaphase plates on meiosis II spindles. In *bub1*$^{\Delta/\Delta}$ oocytes, chromosome segregation commenced before all chromosomes had congressed. Chromosome segregation was also invariably asymmetric in *bub1*$^{\Delta/\Delta}$ oocytes and often accompanied by the appearance of individual chromatids (monads). Meiosis II bipolar spindles formed (albeit longer than normal) despite the highly abnormal meiosis I chromosome segregation, but many of the egg's chromosomes failed to congress to the center of these spindles and instead moved back and forth between the poles in a highly dynamic fashion.

To measure the chromosome congression defects in *bub1*$^{\Delta/\Delta}$ oocytes, the chromosome segregation axis was determined for each individual cell (Figure S1). This was not always possible in *bub1*$^{\Delta/\Delta}$ oocytes and we therefore analyzed only oocytes whose axes could be determined unambiguously and were parallel to the imaging plane. A rectangular box (with a defined size) perpendicular to the segregation axis was positioned in each of the five frames prior to that in which chromosome segregation was first observed. This was done in a manner that maximized the amount of chromosomal DNA contained within the rectangular box. In *BUB1*$^{F/F}$ oocytes, the maximum amount of DNA contained within the box varied very little between 60 min (81.1% ± 12.4%, n = 8) and 12 min (83. 4% ± 6.9%) prior to anaphase I (Figure 2B). This figure is therefore a measure of maximum chromosome density, which is clearly enhanced by the process of chromosome congression. In *bub1*$^{\Delta/\Delta}$ oocytes, the equivalent maxima were merely 51.3% ± 13.9% (n = 8) at 60 min and 42.0% ± 10.1% at 12 min prior to anaphase ($p < 0.001$ at all time points).

To document chromosome missegregation in *bub1*$^{\Delta/\Delta}$ oocytes, we prepared chromosome spreads from *BUB1*$^{F/F}$ and *bub1*$^{\Delta/\Delta}$ oocytes before and after their first meiotic division. Oocytes used for preparing meiosis I spreads were matured in vitro for 2–3 hr after GVBD whereas MII oocytes were obtained directly from hormonally stimulated females. Spreads obtained from *BUB1*$^{F/F}$ (n = 20) and *bub1*$^{\Delta/\Delta}$ oocytes (n = 23) in meiosis I invariably contained 20 bivalent chromosomes. The abnormal chromosome missegregation within *bub1*$^{\Delta/\Delta}$ oocytes cannot therefore be caused by a lack of chiasmata before maturation. As expected, chromosome spreads from MII *BUB1*$^{F/F}$ oocytes (n = 28) invariably contained 20 dyad chromosomes. In contrast, spreads from MII *bub1*$^{\Delta/\Delta}$ oocytes (n = 36) revealed extensive aneuploidy, which was documented with spectral karyotyping (SKY) (Figures 2C and 2D; Table S1). We observed two types of numerical abnormality: cosegregation to the oocyte of both dyads produced by chiasmata resolution and the presence of single chromatids, indicating precocious loss of sister-chromatid cohesion at centromeres. The frequency with which dyads cosegregated varied between chromosomes, ranging from 5% to 30%, as did the fraction of chromatids present as single chromatids. Most of the latter were present as pairs, either two or four copies. These data imply that loss of Bub1 causes two independent types of aberration: first, nondisjunction of whole chromosomes at meiosis I, and second, a failure to hold sister centromeres together after the first meiotic division, which would cause missegregation at meiosis II but not at meiosis I. The finding that MII *bub1*$^{\Delta/\Delta}$ oocytes sometimes contain all four chromatids implies that individual chromosomes can simultaneously suffer both types of aberration. We conclude that Bub1 is important for congression of bivalents on the meiosis I spindle, disjunction of dyads at meiosis I, and persistence of sister-centromere cohesion until meiosis II.

APC/C Is Required for Meiosis I

To address whether the precocious PBE in *bub1*$^{\Delta/\Delta}$ oocytes is due to premature activation of the APC/C, we used mice in which exons 2 to 4 of the gene encoding the APC/C's Apc2 subunit were flanked by *LoxP* sites (*APC2*^{F}). *Zp3-Cre* converted ten out of ten *APC2*^{F} alleles to *apc2*$^{\Delta}$ in the female germline. Moreover, three out of three *APC2*$^{F/F}$ *Zp3-Cre* females failed to become pregnant when kept with wild-type males for 3 months or more. APC/C activity within oocytes is therefore essential. We observed in some but not all crosses that *APC2*$^{F/F}$ *Zp3-Cre* females possessed many fewer GV oocytes than did their *APC2*$^{F/F}$ littermates. The reason for this is that most oocytes had clearly already undergone GVBD in vivo. Ovary dissection revealed 9 GV and 28 GVBD oocytes from a *APC2*$^{F/F}$ *Zp3-Cre* female and 12 GV and 22 GVBD oocytes from a *BUB1*$^{F/F}$ *APC2*$^{F/F}$ *Zp3-Cre* female, even when dissection was performed in 5 times the normal concentration of IBMX. In contrast, a *BUB1*$^{F/F}$ *APC2*$^{F/F}$ littermate produced 41 GV and no GVBD oocytes. Importantly, of those *apc2*$^{\Delta/\Delta}$ GV oocytes that underwent GVBD only upon removal of IBMX, none underwent PBE (Figure 3A). The APC/C is therefore essential for the first meiotic division, as previously suggested [28]. It is very possibly also important for holding oocytes in prophase prior to GVBD [29].

A Quantitative Assay for APC/C Activity in Oocytes

One of the APC/C's key substrates is securin, whose destruction can be visualized in oocytes by injecting moderate amounts of mRNA encoding fluorescently tagged securin (securin-EGFP) [23, 30–32]. To test whether destruction is mediated by the APC/C, we used confocal microscopy to measure securin-EGFP fluorescence after injection of *apc2*$^{\Delta/\Delta}$ or *APC2*$^{F/F}$ GV oocytes. Neither the first meiotic division nor the rapid drop of securin-EGFP levels (Figure 3B) that precedes PBE in *APC2*$^{F/F}$ oocytes (Figure 3D) took place in *apc2*$^{\Delta/\Delta}$ oocytes. Instead, levels increased continuously for 24 hr, eventually approaching a plateau as the rate of increase gradually declined (Figure 3C). Bivalent chromosomes (marked with histone H2B-cherry) congressed to a metaphase plate but were not converted to dyads and no polar bodies were extruded (Figure 3B).

Because injection of securin-EGFP mRNA had no effect on the timing of PBE in wild-type oocytes, even at the highest levels (Figure S2), its destruction can be used as a marker for the proteolysis of endogenous securin. The rate of APC/C-dependent securin-EGFP proteolysis should be derivable from the first differential (slopes) of EGFP accumulation curves. The rate of change of securin mRNA (M) and protein (S) can be described by two differential equations (DE):

$$\frac{dM}{dt} = -k_d^m \cdot M$$

$$\frac{dS}{dt} = k_S \cdot M - \left(k_d' + k_d \cdot APC\right) \cdot S$$

Degradation of securin mRNA (M) is assumed to be first order, with rate constant k_d^m ($time^{-1}$). Securin synthesis (i.e., translation) is described by the first term in the securin DE ($k_S \cdot M$) whereas its degradation is described by APC/C-independent (k_d') and APC/C-dependent ($k_d \cdot APC$) terms. APC refers to active APC/C concentration and k_d to its specific activity or turnover rate. Because these cannot be estimated

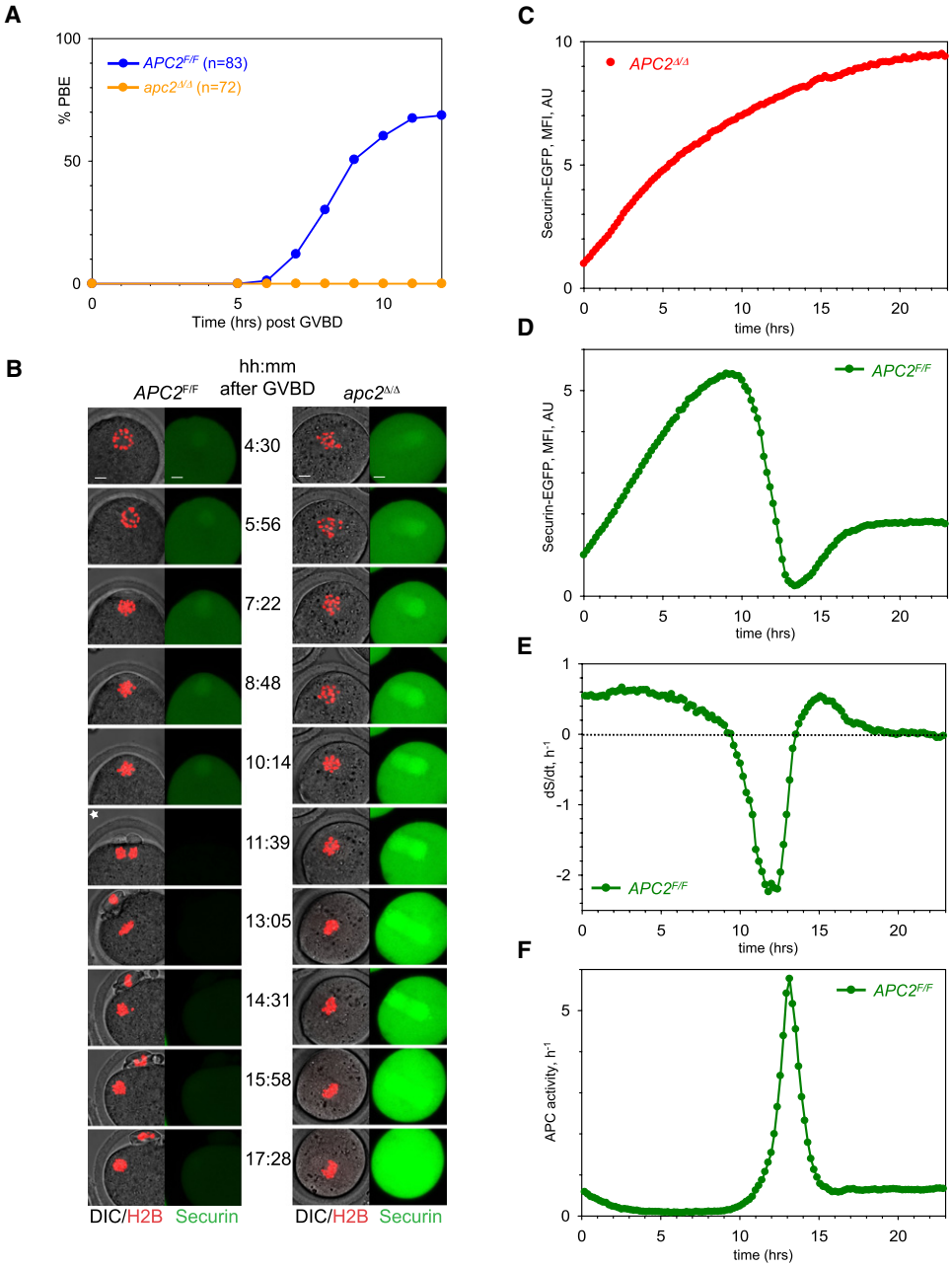

Figure 3. Calculation of APC/C Activity from Securin Level Changes in *APC2*$^{F/F}$ and *apc2*$^{\Delta/\Delta}$ Oocytes

(A) Kinetics of polar body extrusion (PBE) in *APC2*$^{F/F}$ and *apc2*$^{\Delta/\Delta}$ oocytes. *APC2*$^{F/F}$ and *apc2*$^{\Delta/\Delta}$ oocytes were harvested in M2 medium containing IBMX, which inhibits GVBD. Oocytes were released into inhibitor-free M16 medium. 90 min after release those oocytes that had completed GVBD were selected for further analysis. This was set as time = 0 hr. Oocytes were monitored every hour and scored for completion of PBE.

(B) Images from movies with *APC2*$^{F/F}$ and *apc2*$^{\Delta/\Delta}$ oocytes expressing H2B-mCherry and securin-EGFP. Observe that securin does not get degraded in the absence of Apc2.

(C and D) Securin-EGFP levels in *apc2*$^{\Delta/\Delta}$ (C) and in *APC2*$^{F/F}$ (D) oocytes were measured at each time point and background levels were subtracted. Values were normalized relative to that at GVBD (0 hr), and plotted, in arbitrary units (AU), against time.

(E) The first derivative (dS/dt) of the Securin level curve (Figure 2C) in *APC2*$^{F/F}$ oocytes.

(F) Changes in APC/C activity during meiotic maturation in *APC2*$^{F/F}$ oocytes. See details in the text.

separately, we simply refer to $k_d \cdot APC$ as APC/C activity. The key point is that this is not constant during oocyte maturation, with a large rise being responsible for the rapid drop in securin levels shortly before PBE. Importantly, $k_d \cdot APC$ can be calculated at each time point from the temporal pattern of its substrate (securin-EGFP) levels. Thus:

$$k_d \cdot APC = \frac{k_S \cdot M_0 \cdot e^{-k_d^m \cdot t} - \frac{dS}{dt}}{S} - k_d'$$

where M_0 is the level of injected securin mRNA and $k_S \cdot M_0$ is the maximal rate of securin mRNA translation. Calculation of

APC/C activity requires values for kinetic rate constants ($k_S \cdot M_0$, k_d', and k_d^m), the securin-EGFP level (S), and its rate of change (dS/dt, which is the slope of the securin curve).

The securin accumulation data in *apc2*$^{\Delta/\Delta}$ oocytes do not provide any information about the stability of securin mRNA (k_d^m), but it turns out that this can be estimated from changes in securin-EGFP levels in *APC2*$^{F/F}$ oocytes, where the time derivative of securin levels (dS/dt) becomes positive again (because of mRNA translation) after APC/C-dependent securin degradation during anaphase of MI (Figure 3E). Importantly, the maximal value of dS/dt is greater than 80% of its value at GVBD (15 hr previously), implying that the rate of mRNA degradation is negligible. We therefore assumed that $k_d^m = 0$.

The kinetic parameters, $k_S \cdot M_0 = 1.05\ h^{-1}$ and $k_d' = 0.1\ h^{-1}$, were estimated (see Figure S3) from the securin-EGFP data of *apc2*$^{\Delta/\Delta}$ oocytes (Figure 3C), where $k_d' \cdot$APC is zero. With these kinetic parameters in hand, we can use values of S (Figure 3D) and dS/dt (Figure 3E) to calculate APC/C activity during meiotic progression (Figure 3F). Because the dominating terms are the securin levels (S) and its time derivative (dS/dt), the activities calculated are in fact quite insensitive to the precise kinetic parameter values. APC/C activity was also calculated assuming Michaelis-Menten rather than first-order degradation kinetics for securin (Figure S4).

These calculations reveal that APC/C activity relaxes rapidly to zero after GVBD, remains at this low level until about 10 hr after GVBD, increases dramatically shortly before the first meiotic division, and then drops back to a low but nonzero value (Figure 3F). Unlike peak levels during MI, resting APC/C activity during CSF arrest is sensitive to the value of k_d^m: the higher the rate of mRNA degradation, the lower the implied APC/C activity. Importantly, kinetic parameter combinations consistent with zero APC/C activity in MII are unrealistic because they predict negative APC/C activity during meiotic progression. We are therefore confident that APC/C activity against securin is not completely turned off during MII CSF arrest. Incomplete inhibition by Emi2 could be responsible for the gradual turn-over of cell cycle regulators at this stage of the meiotic process [33].

Premature APC/C Activation in *bub1*$^{\Delta/\Delta}$ Oocytes

To test whether APC/C activation precedes precocious chromosome segregation in oocytes lacking Bub1, we imaged oocytes from *BUB1*$^{F/F}$ *Zp3-Cre* and *BUB1*$^{F/F}$ females after their injection with securin-EGFP and histone H2B-cherry mRNAs (Figures 4A and 4B; Movie S1). In *BUB1*$^{F/F}$ oocytes, APC/C activity reaches a maximum at the time of chromosome segregation (Figure 4C, green arrowheads), about 12 hr after GVBD. The kinetics of the rise and fall of APC/C activity was similar in *bub1*$^{\Delta/\Delta}$ oocytes, but strikingly the burst of APC/C activity occurred 4–5 hr earlier. The implication is that Bub1 is necessary to inhibit APC/C activity for a large fraction of the period between GVBD and PBE. To our surprise, we found that Bub1 causes a similar delay in APC/C activity toward cyclin A-GFP (Figure S5).

Individual activity curves were aligned and an average activity curve calculated (Figure 4D). This reveals that there is little or no significant difference in maximal APC/C activity between *BUB1*$^{F/F}$ and *bub1*$^{\Delta/\Delta}$ oocytes, the only difference being the timing of the meiosis I burst of activity. It also shows that APC/C activity rises in an exponential fashion for 3–4 hr in *BUB1*$^{F/F}$ and *bub1*$^{\Delta/\Delta}$ oocytes (Figure 4E). There was a small difference in their exponents (−0.66 in the mutant versus −0.84 in the wild-type), implying a slightly more "explosive" activation in *BUB1*$^{F/F}$ than in *bub1*$^{\Delta/\Delta}$ oocytes. Interestingly, the period of exponential increase lasted nearly 4 hr in both sets of oocytes.

Premature Chiasmata Resolution in *bub1*$^{\Delta/\Delta}$ Oocytes Depends on APC/C and Separase

Many events are advanced by 4–5 hr in *bub1*$^{\Delta/\Delta}$ oocytes. Some are normally associated with the first meiotic division, namely securin destruction, chiasmata resolution, and PBE, whereas others such as loss of centromeric cohesion normally only take place at the second meiotic division. Temporal dislocation on this scale has hitherto not been documented in SAC mutants and it was therefore important to address whether premature activation of the APC/C (and thereby separase) was responsible. Because the tripeptide proteasome inhibitor MG132 was found to depress securin-EGFP synthesis (Figure S6), we addressed the APC/C's role by analyzing oocytes from *Bub1*$^{flox/flox}$*Apc2*$^{flox/flox}$ *Zp3-Cre* females, in which both Apc2 and Bub1 are depleted. The phenotype of such oocytes was similar, though not identical to those from *Apc2*$^{flox/flox}$ *Zp3-Cre* females. They did not extrude polar bodies and, after injection of securin-EGFP mRNAs, accumulated EGFP fluorescence in an asymptotic fashion over a 20 hr period (Figure 5A and data not shown). Congression of bivalents was, however, inefficient and they did not form compact metaphase plates (Figure 5B). Despite this, many if not most bivalents clearly came under tension, indicating biorientation of maternal and paternal kinetochores (Figure 5C). Importantly, chiasmata were not resolved (Figure 5C). Precocious APC/C activity must therefore be responsible for many of the phenotypes caused by Bub1 depletion. It is difficult to know whether the defective congression of bivalents in *apc2*$^{\Delta/\Delta}$ *bub1*$^{\Delta/\Delta}$ oocytes was exclusively due to depletion of Bub1 because congression also appeared somewhat abnormal in *apc2*$^{\Delta/\Delta}$ oocytes (Figure 5B).

To address whether the precocious resolution of chiasmata in *bub1*$^{\Delta/\Delta}$ oocytes is due to premature activation of separase as opposed to other activities capable of destroying sister-chromatid cohesion [34], we analyzed oocytes from *Bub1*$^{flox/flox}$ *separase*$^{flox/flox}$ *Zp3-Cre* females, in which both Bub1 and separase are depleted. Inactivation of separase did not alter precocious APC/C activation (Figure 5E) but it did hinder PBE (Figure 5D). 92.3% of *bub1*$^{\Delta/\Delta}$ oocytes (n = 36) extruded a polar body at an average time of 05:34 ± 01:53 hr post GVBD (n = 36) but only 14.9% of *sep*$^{\Delta/\Delta}$ *bub1*$^{\Delta/\Delta}$ oocytes did so, with an average time of 07:00 ± 04:44 hr (n = 46). Live imaging of *sep*$^{\Delta/\Delta}$ *bub1*$^{\Delta/\Delta}$ oocytes injected with securin-EGFP and histone H2B-cherry showed that many bivalents came under tension, even after securin had been fully destroyed, presumably because chiasmata had not been resolved (data not shown). To confirm this, we prepared chromosome spreads from *bub1*$^{\Delta/\Delta}$ and *sep*$^{\Delta/\Delta}$ *bub1*$^{\Delta/\Delta}$ oocytes at various times after GVBD, starting from when at least 90% of *bub1*$^{\Delta/\Delta}$ oocytes had completed PBE. All bivalents had been converted to dyads or single chromatids in 100% (n = 66) of *bub1*$^{\Delta/\Delta}$ oocytes but never (n = 79) in *sep*$^{\Delta/\Delta}$ *bub1*$^{\Delta/\Delta}$ oocytes (Figure 5F), even long after APC/C activation.

The Oocyte SAC Does Not Require the Bub1 Kinase Domain

Injection of *bub1*$^{\Delta/\Delta}$ oocytes with wild-type Bub1 but not with a frame-shifted (NS-Bub1) mRNA delayed both APC/C activation (compare Figure 6A with Figure 4D) and PBE, causing both events to occur with a timing similar to that of *BUB1*$^{F/F}$

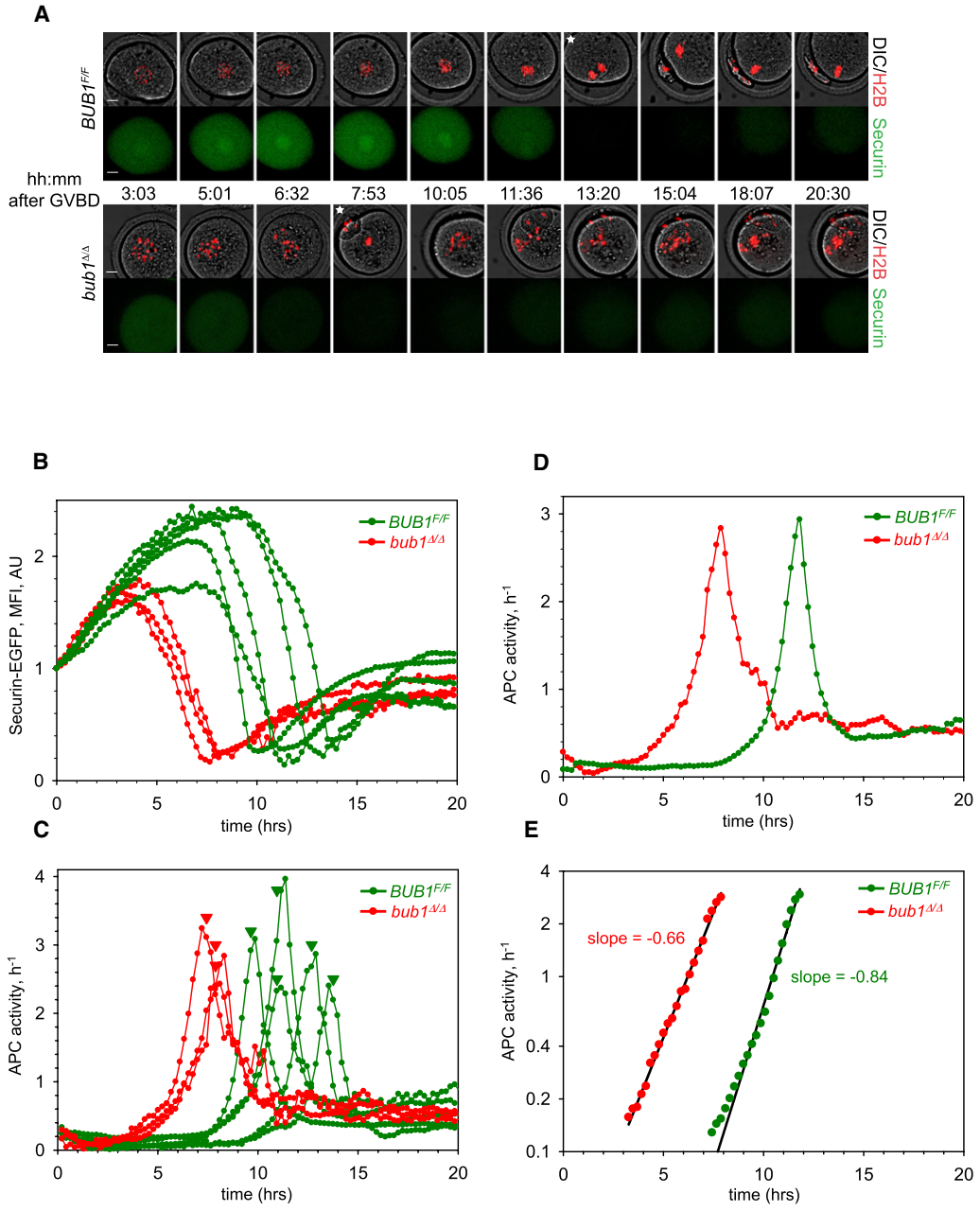

Figure 4. Premature Activation of the APC/C in *bub1*$^{\Delta/\Delta}$ Oocytes

Chromosome movements and securin levels in *BUB1*$^{F/F}$ and *bub1*$^{\Delta/\Delta}$ oocytes expressing H2B-mCherry and securin-EGFP were observed by time-lapse confocal microscopy.

(A) Still images from a representative movie of each genotype are shown. The upper panels show DIC images merged with the H2B-mCherry channel pseudocolored in red. The lower panels show the securin-EGFP channel pseudocolored in green. The asterisks indicate the frame where chromosome segregation was first observed. Scale bars represent 10 μm.

(B) Securin-EGFP levels in movies similar to those shown in (A) were measured at each time point and background levels were subtracted. Values were normalized relative to that at GVBD (0 hr), and plotted, in arbitrary units (AU), against time. Movies were aligned relative to time of GVBD.

(C) The securin-EGFP curves in (B) were transformed to produce a measure of APC/C activity over the course of the experiment (see text) and plotted against time.

(D) The APC/C-activity curves in (C) were aligned relative to the average time to peak APC/C activity for each genotype, and the average APC/C activity at each time point was calculated and plotted against time.

(E) The exponentially rising portions of the average APC/C-activity curves shown in (D) were plotted on a semilog plot, and a line of best fit was projected onto the data. The slopes of the lines are indicated on the graph.

oocytes (data not shown). To address the function of Bub1's conserved kinase domain, GV-stage *bub1*$^{\Delta/\Delta}$ oocytes were injected with mRNAs encoding H2B-cherry and securin-EGFP together with either wild-type Bub1 mRNA, NS-Bub1 mRNA, or an mRNA encoding a version of Bub1 lacking its C-terminal kinase domain (Bub1-KinΔ). Time-lapse confocal movies (data

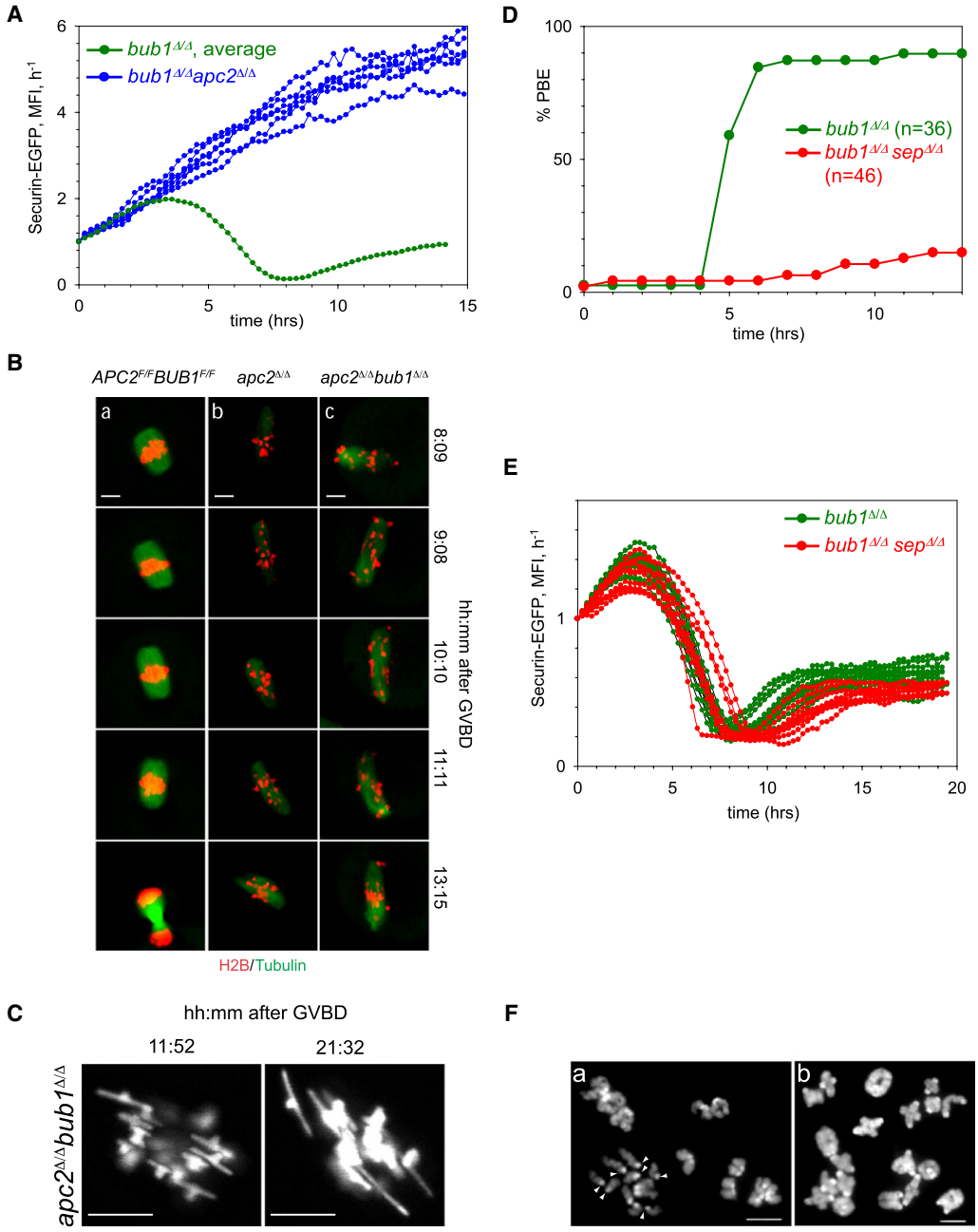

Figure 5. Separase and Apc2 Are Required for Precocious Chromosome Segregation and PBE in *bub1*$^{\Delta/\Delta}$ Oocytes

(A) Chromosome movements and securin levels in *bub1*$^{\Delta/\Delta}$ and *apc2*$^{\Delta/\Delta}$ *bub1*$^{\Delta/\Delta}$ oocytes expressing H2B-mCherry and securin-EGFP were observed by time-lapse confocal microscopy. Securin-EGFP levels were measured at each time point and plotted against time as previously. Movies were aligned relative to time of GVBD. Note the *bub1*$^{\Delta/\Delta}$ curve is the average of five individual oocytes.

(B) Chromosome movements and microtubule spindle dynamics were visualized by time-lapse confocal microscopy in three types of oocytes expressing histone H2B-mCherry and β-Tubulin-EGFP: (a) *APC2*$^{F/F}$ *BUB1*$^{F/F}$, (b) *apc2*$^{\Delta/\Delta}$, and (c) *apc2*$^{\Delta/\Delta}$ *bub1*$^{\Delta/\Delta}$. Still images from a representative movie of each genotype are shown. The merged H2B-mCherry and β-Tubulin-EGFP channels are shown pseudocolored in red and green, respectively. Scale bars represents 10 μm.

(C) Representative still images, taken at 11.87 hr and 21.54 hr after GVBD, from the chromatin (H2B-mCherry) channel shows highly stretched bivalents from an *apc2*$^{\Delta/\Delta}$ *bub1*$^{\Delta/\Delta}$ oocyte.

(D) Kinetics of polar body extrusion (PBE). *bub1*$^{\Delta/\Delta}$ and *bub1*$^{\Delta/\Delta}$ *separase*$^{\Delta/\Delta}$ oocytes were harvested in M2 medium containing IBMX, which inhibits GVBD. Oocytes were released into inhibitor-free M16 medium. 90 min after release, those oocytes that had completed GVBD were selected for further analysis. This was set as time = 0 hr. Oocytes were monitored every hour and scored for completion of PBE.

(E) Chromosome movements and securin levels in *bub1*$^{\Delta/\Delta}$ (n = 11) and *bub1*$^{\Delta/\Delta}$ *separase*$^{\Delta/\Delta}$ (n = 12) oocytes expressing H2B-mCherry and securin-EGFP were observed by time-lapse confocal microscopy. Securin-EGFP levels were measured at each time point and plotted against time as previously. Movies were aligned relative to time of GVBD.

(F) *bub1*$^{\Delta/\Delta}$ and *bub1*$^{\Delta/\Delta}$ *separase*$^{\Delta/\Delta}$ oocytes were harvested at GV stage and matured in vitro for up to 22 hr. Chromosome spreads were prepared when at least 90% of *bub1*$^{\Delta/\Delta}$ oocytes had completed MI, but not MII, as judged by extrusion of the first polar body. Only those *bub1*$^{\Delta/\Delta}$ oocytes that had completed

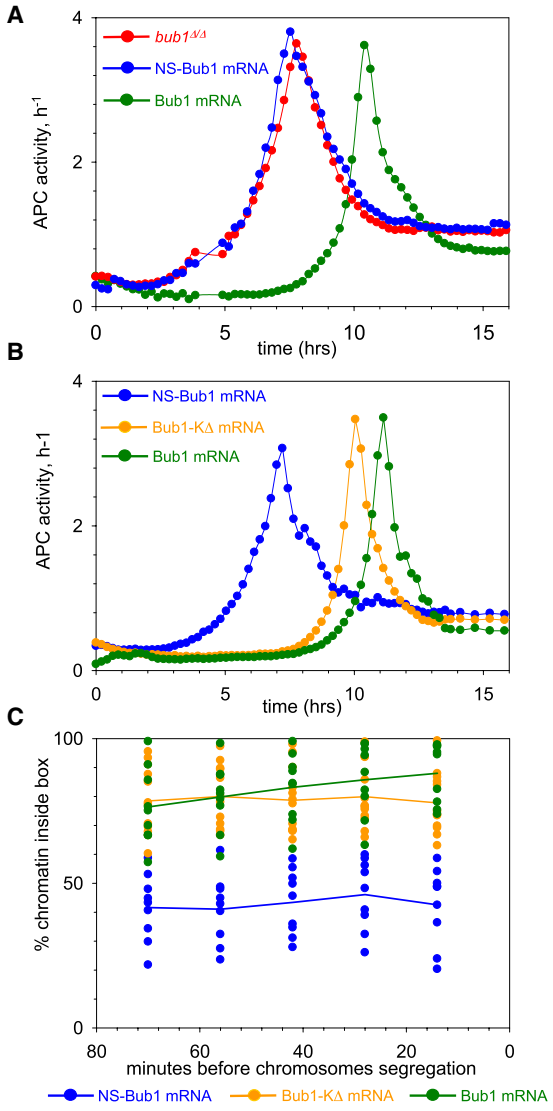

Figure 6. Bub1 Kinase Domain Is Largely Dispensable for the Spindle Assembly Checkpoint in Oocytes

(A) Chromosome movements and securin levels in *bub1*$^{\Delta/\Delta}$ oocytes expressing H2B-mCherry and securin-EGFP were observed by time-lapse confocal microscopy. A subset of the oocytes was also microinjected with Bub1 mRNA, a further subset was microinjected with NS-Bub1 mRNA, and the remainder were not microinjected with Bub1 mRNA. Securin-EGFP levels were measured at each time point and average APC/C activity curves for each group of oocytes were calculated and plotted against time as previously.

(B) As in (A) except the third group was also microinjected with mRNA for a Bub1 kinase-deletion mutant (Bub1-KΔ).

(C) The oocytes described in (A) and (B) were analyzed as in Figure 2B to measure the extent of chromosome congression.

not shown) demonstrated that the (average) interval between GVBD and PBE with wild-type Bub1 mRNA was 11:07 ± 01:08 hr (n = 10). It was 07:15 ± 00:38 hr (n = 9) with NS-Bub1 mRNA and 10:07 ± 01:02 hr (n = 14) with Bub1-KinΔ mRNA. The difference between NS-Bub1 and wild-type was statistically significant ($p < 0.001$) as was that between NS-Bub1 and Bub1-KinΔ ($p < 0.001$). Though the error bars overlap considerably, the small difference in timing between oocytes injected with wild-type and Bub1-KinΔ mRNA appears to be real, with $p = 0.041$.

Securin-EGFP levels were quantified and transformed into APC/C activity curves that were then aligned and averaged (Figure 6B). The average interval from GVBD to peak APC/C activity was 07:20 ± 00:43 hr with NS-Bub1 mRNA, 11:02 ± 01:03 hr with wild-type Bub1 mRNA, and 10:04 ± 01:04 hr with Bub1-KinΔ mRNA. The differences between Bub1-KinΔ and NS-Bub1 mRNA was highly significant ($p < 0.001$) whereas the difference between wild-type and Bub1-KinΔ was less so ($p = 0.039$). These data suggest that much of the delay in APC/C activation resulting from Bub1 can also be performed by a version completely lacking its kinase domain. Indeed, the shape of the APC/C activation curves is very similar with and without Bub1's kinase domain (Figure 6B). This domain is nevertheless highly conserved and appears from our data to enhance Bub1's ability to regulate (delay) APC/C activation and anaphase onset.

Wild-type Bub1 and Bub1-KinΔ but not NS-Bub1 mRNA ($p < 0.001$) restored chromosome congression in *bub1*$^{\Delta/\Delta}$ oocytes to wild-type levels (compare Figure 6C with Figure 2B). There was, however, a small statistically significant difference between wild-type and KinΔ mRNAs at the final time point, 14 min prior to segregation. The kinase activity of Bub1 can only have a minor function, if any, in regulating chromosome congression.

Discussion

The notion that the SAC may be unimportant or ineffective in oocytes still persists [35] despite evidence to the contrary [19, 21, 24, 25, 36]. We describe here the consequences of depleting a key SAC component, namely Bub1, by oocyte-specific deletion of a floxed allele of the *BUB1* gene. This adversely affects chromosome congression, advances chiasmata resolution and polar body extrusion by 4–5 hr, and causes precocious separation of sister centromeres. By using a quantitative assay for APC/C activity and analyzing the phenotypes of double mutants, we show that the precocious chiasmata resolution and PBE caused by loss of Bub1 is accompanied by and depends on premature activation of the APC/C and separase. Our data prove that the SAC has a fundamental role in regulating anaphase in oocytes and that it largely performs this function independently of Bub1's kinase domain.

Our measurements show that APC/C's activity toward securin remains very low from GVBD until 3 hr before PBE, at which point it rises at an exponential rate, peaking shortly before PBE, before declining to a low but significant level during CSF arrest. There are two possible explanations for the exponential APC/C activation (suggestive of an autocatalytic process). Given that the SAC depresses APC/C activity during the process of exponential activation in wild-type oocytes, it is

the first PBE were spread whereas all *bub1*$^{\Delta/\Delta}$ *separase*$^{\Delta/\Delta}$ oocytes were spread. Chromosome spreads were stained with DAPI to visualize DNA and resolution of chiasmata was scored as (a) positive or (b) negative. (a) shows a spread from a *bub1*$^{\Delta/\Delta}$ oocyte. Again, separated sister chromatids were observed (indicated by arrowheads). (b) shows a spread from a *bub1*$^{\Delta/\Delta}$ *separase*$^{\Delta/\Delta}$ oocyte. Note, chromosomes from *bub1*$^{\Delta/\Delta}$ oocytes were generally too widely dispersed on the slide to capture all chromosomes in a single image. The visible chromosomes from a single spread were photographed in a number of separate images at the same magnification; these images were subsequently arranged in proximity to one another to produce the images shown above. Scale bars represent 10 μm.

conceivable that APC/C activity inactivates a SAC component, such as Mad2 [37, 38] or Mps1 [39] and/or Aurora B [9] kinases. Alternatively, the exponential rise in the rate of securin destruction could come about because of competition with a competing APC/C substrate whose destruction must precede that of securin. Cyclin A might be such a protein. However, we found no major difference in the kinetics of securin and cyclin A destruction (see Figure S5).

If inactivation of the SAC drives APC/C activation in wild-type oocytes, what process does so in oocytes lacking Bub1? More precisely, what changes occur in *bub1*$^{\Delta/\Delta}$ oocytes during the 7 hr interval between GVBD, when cyclin B/Cdk1 is presumably activated, and the complete activation of the APC/C fully 7 hr later? Phosphorylation of several APC/C subunits accompanies its activation in mitotic cells [40, 41], though the physiological significance of this phosphorylation has not been addressed. It is conceivable that a battle between mitotic kinases and phosphatases takes place during this period, with the former finally triumphing. Our finding that the process of APC/C activation is exponential in *bub1*$^{\Delta/\Delta}$ oocytes potentially adds a new player, namely the APC/C itself, which might activate itself via a positive feedback loop. We note that the variation in time between GVBD and full APC/C activation in *bub1*$^{\Delta/\Delta}$ oocytes (38 min) was half that in wild-type ones (74 min). Presumably, the process activating the APC/C without a SAC is not subject to the vagaries of the stochastic process of kinetochore capture and biorientation. How might the APC/C promote its own activation? It has been suggested that inhibition of APC/C mediated ubiquitinylation of securin because its phosphorylation by Cdk1 makes the process more switch-like in yeast [42]. This model cannot account for the switch-like nature of securin destruction in oocytes because separase, a key part of the yeast autoactivation process, is not required for the exponential rise in APC/C activity in oocytes lacking both Bub1 and separase (data not shown).

Another function of the APC/C revealed by this work stems from our finding that oocytes whose Apc2 subunit has been depleted during their growing phase appear to re-enter the meiotic program precociously, apparently undergoing GVBD en masse within the ovary. This raises the possibility that the APC/C is at least partially active during the long prophase arrest in oocytes and that without it oocytes are more likely to re-enter the first meiotic division, possibly in the absence of the luteinizing hormone surge that normally induces this event. A related phenomenon, though one whose physiological significance is less clear, is the recent finding that antisense morpholinos directed against Cdh1 mRNA permit a fraction of GV oocytes to undergo GVBD in vitro in the presence of phosphodiesterase inhibitors that normally block this process [29]. The importance of molecular mechanisms controlling prophase I arrest in oocytes during folliculogenesis was recently demonstrated by disruption of PTEN, a regulator of phosphatidylinositol 3-kinase, which caused a reduction of the oocyte pool at an early age leading to premature ovarian failure (POF) [43]. In *apc2*$^{\Delta/\Delta}$ oocytes we have observed a similar effect and it is therefore conceivable that disruption of normal APC/C activity in growing oocytes might contribute to POF.

Our data suggest that Bub1 may have at least two other functions within oocytes besides delaying APC/C activation, namely to facilitate congression of bivalents on meiosis I spindles and prevent premature destruction of sister-centromere cohesion. It is important to point out that we cannot at this stage be certain that the congression and cohesion defects are not at least partly caused by the premature APC/C activation. It is easy to imagine that by giving cells less time to biorient bivalents, premature APC/C activation would by itself hinder their congression. It is less easy to imagine why it would hinder the mechanism that normally protects sister-chromatid cohesion at centromeres from separase during meiosis I. The precocious separation of sister centromeres in *bub1*$^{\Delta/\Delta}$ oocytes is reminiscent of the situation during meiosis I in yeast where Bub1 is necessary for the recruitment to centromeres of shugoshin proteins (e.g., Sgo1) that protect cohesin from separase [44–46]. Bub1 might act in a similar fashion in oocytes, helping to recruit Sgo1 or Sgo2 to centromeres. Because the precocious loss of sister-chromatid cohesion at centromeres in *bub1*$^{\Delta/\Delta}$ oocytes is not fully penetrant, afflicting less than one-third of all chromosomes, there must also exist a mechanism conferring protection that is Bub1 independent.

In the light of our finding that the SAC delays APC/C activation by 4 to 5 hr, the massive missegregation in aging human females cannot be attributed to an inherently ineffective SAC in oocytes. It is nevertheless conceivable that the SAC might work less effectively as oocytes ages and that this facilitates production of aneuploid gametes. It is also important to point out that our work does not address whether the delay in APC/C activation caused by Bub1 involves signaling from kinetochores that have not yet attached to microtubules. Indeed, it remains mysterious why univalent X chromosomes fail to block meiosis I in mouse oocytes. It seems implausible that oocytes would possess a SAC that cannot monitor the correct attachment of individual chromosomes and yet univalent X chromosomes apparently do not greatly delay APC/C activation. A recent study has shown that the sister kinetochores of univalent chromosomes in meiosis I oocytes can become bioriented on the meiosis I spindle, apparently satisfying the requirements of the SAC and contributing to chromosome missegregation [36]. Further insight into this process could be gained by monitoring activity of the APC/C and the actual movement of univalent chromosomes during meiosis I using the sort of techniques described in this paper.

Experimental Procedures

Mouse Strains

Generation of *BUB1*$^{F/F}$ [14], *SEPARASE*$^{F/F}$ [47], and *APC2*$^{F/F}$ [48] mice has been described previously. A transgenic mouse line that expresses Cre recombinase from the Zona pellucida 3 promoter (Zp3-cre) [26] was purchased from the Jackson Laboratory. Mouse strains used were of mixed C57BL/6J and 129/Sv backgrounds.

Oocyte Culture and Microinjection

Fully grown mouse GV-stage oocytes surrounded by cumulus cells were isolated by disaggregating ovaries in M2 medium (Specialty Media, Millipore, Watford, UK, or Sigma-Aldrich) supplemented with 200 mM 3-isobutyl-1-methylxanthine (IBMX, Sigma-Aldrich) at 37°C. Oocytes released from most of the surrounding cumulus cells were cultured in drops of medium (~50 μl) covered with mineral oil (Sigma-Aldrich). Oocytes were matured in M16 medium (Specialty Media) at 37°C in the presence of 5% CO_2. Only oocytes that had undergone GVBD (germinal vesicle breakdown) within 90 min after release into IBMX-free medium were selected (time 0 hr after GVBD) and cultured further for experiments. In experiments where oocytes were cultured in medium containing nocodazole at 5 μM or MG132 at 10 μM, controls were treated with an equivalent amount of ethanol or DMSO solvent, respectively. MII-arrested oocytes were obtained from females superovulated by intraperitoneal (i.p.) injection of PMSG (5 IU) followed 48 hr later by i.p. injection of human chorionic gonadotropin (hCG; 5 IU). Oocytes were isolated from oviducts approximately 16 hr after hCG and freed from cumulus cells by hyaluronidase (200 IU/ml, Sigma-Aldrich). GV oocytes were microinjected in M2 media supplemented with IBMX with a FemtoJet microinjector (Eppendorf) with 5–10 pl of mRNAs at a final

concentration of 0.1 μg/ml in RNase-free water (Ambion) into the cytoplasm. Up to two different mRNAs were mixed together prior to injection. Control and experimental oocytes for a single experiment were imaged simultaneously, distinguished by coinjection of 10 kDa Cascade-Blue-labeled dextran into one group. After approximately 1–2 hr to allow for protein expression, oocytes were matured.

Chromosome Spreads

Chromosome spreads from mouse oocytes were prepared as previously described [49, 50]. See Supplemental Data for further details.

SKY Analysis

BUB1$^{F/F}$ and *BUB1*$^{\Delta/\Delta}$ mice were primed with 5IU PMSG, then 48 hr later with 5IU hCG, and oviducts were isolated 16–18 hr after hCG. The cumulus-enclosed oocytes at the second meiotic division (MII) were released into M2 medium with 1% hyaluronidaze for 5–10 min. Cumulus-free oocytes were fixed in methanol-acetic acid solution (3:1). Slides were aged for 2–3 days at the room temperature and then hybridized with the SKY probe (Applied Spectral Imaging) according to the manufacturer's instructions. SKY image acquisition and analysis was performed on a Zeiss Axioscope 2 microscope equipped with SpectraCubeTM at 600× with Spectral Imaging Expo 2.6 software.

Live Imaging and Quantitative Analysis of Data

Oocytes were cultured in a PeCon (Erbach, Germany) environmental microscope incubator allowing the maintenance of a 5% CO_2 atmosphere with humidity at 37°C during time-lapse experiments. A customized Zeiss LSM510 META confocal microscope equipped with Plan-Neofluor 20×/0.5, C-Apochromat 40×/1.2 NA water immersion or C-Apochromat 40×/1.2 NA water immersion objective lenses was used for image acquisition. For detection of Cascade-Blue dextran, EGFP, YFP, and mCheery, we used 405 nm, 488 nm, 514 nm, and 561 nm excitation wavelengths and LP 420, BP 505-550, BP 530-600, and LP 575 filters. Chromosomes labeled with H2B-mCherry were tracked with an EMBL-developed tracking macro [51] adapted to our microscope. Image stacks were captured every 12–15 min for 16–20 hr. Quantitative analysis of the density of the fluorescence was performed with ImageJ software (http://rsb.info.nih.gov/ij/). To measure securin-EGFP signal, the area occupied by the oocyte in each individual frame was defined manually and the mean fluorescence intensity (MFI) of the signal within this area was measured. Values were corrected for background fluorescence by subtracting the MFI of the area surrounding the oocyte at each time point. To control for the apparent differences in MFI levels between individual oocytes caused by discrepancies in the amount of injected mRNA, background-corrected MFI values were normalized to the value measured at the time of GVBD. The changes in APC/C activity (kd.APC) during meiosis were calculated from the securin-EGFP signal with MS Excel. The time derivative of the Securin curve (dS/dt) was approximated by the ratio of differences ($\Delta S/\Delta t$) of subsequent time points. In order to reduce noise in the ratio of differences, the securin data were smoothed by calculating the average of three subsequent points (a three-point running mean).

DNA Constructs, Primers, mRNA Synthesis, and Statistical Analysis

See Supplemental Data.

Supplemental Data

Supplemental Data include Supplemental Experimental Procedures, six figures, one table, and two movies and can be found with this article online at http://www.current-biology.com/supplemental/S0960-9822(09)00685-X.

Acknowledgments

We are grateful to Jan Ellenberg and Melina Schuh for their help with live imaging of oocytes, Denise Jelfs for technical assistance, Katja Wassmann, Melina Schuh, and Nathalie Daigle for DNA plasmids, and all members of the Nasmyth lab for helpful discussions. M.A. was supported by EC Fellowship MEIF-CT-2005-024429 and by BBSRC through OCISB and GAAV no. IAA501620801.

Received: December 1, 2008
Revised: January 28, 2009
Accepted: January 29, 2009
Published online: February 26, 2009

References

1. Vogt, E., Kirsch-Volders, M., Parry, J., and Eichenlaub-Ritter, U. (2008). Spindle formation, chromosome segregation and the spindle checkpoint in mammalian oocytes and susceptibility to meiotic error. Mutat. Res. *651*, 14–29.
2. Mitchison, T.J., and Salmon, E.D. (2001). Mitosis: a history of division. Nat. Cell Biol. *3*, E17–E21.
3. Nicklas, R.B. (1967). Chromosome micromanipulation. II. Induced reorientation and the experimental control of segregation in meiosis. Chromosoma *21*, 17–50.
4. Nasmyth, K., and Haering, C.H. (2005). The structure and function of SMC and kleisin complexes. Annu. Rev. Biochem. *74*, 595–648.
5. Uhlmann, F., Wernic, D., Poupart, M.A., Koonin, E., and Nasmyth, K. (2000). Cleavage of cohesin by the CD clan protease separin triggers anaphase in yeast. Cell *103*, 375–386.
6. Waizenegger, I., Hauf, S., Meinke, A., and Peters, J.M. (2000). Two distinct pathways remove mammalian cohesin from chromosome arms in prophase and from centromeres in anaphase. Cell *103*, 399–410.
7. Stemmann, O., Zou, H., Gerber, S.A., Gygi, S.P., and Kirschner, M.W. (2001). Dual inhibition of sister chromatid separation at metaphase. Cell *107*, 715–726.
8. Peters, J.M. (2006). The anaphase promoting complex/cyclosome: a machine designed to destroy. Nat. Rev. Mol. Cell Biol. *7*, 644–656.
9. Taylor, S., and Peters, J.M. (2008). Polo and Aurora kinases: lessons derived from chemical biology. Curr. Opin. Cell Biol. *20*, 77–84.
10. Musacchio, A., and Salmon, E.D. (2007). The spindle-assembly checkpoint in space and time. Nat. Rev. Mol. Cell Biol. *8*, 379–393.
11. Li, R., and Murray, A.W. (1991). Feedback control of mitosis in budding yeast. Cell *66*, 519–531.
12. Buffin, E., Emre, D., and Karess, R.E. (2007). Flies without a spindle checkpoint. Nat. Cell Biol. *9*, 565–572.
13. Michel, L.S., Liberal, V., Chatterjee, A., Kirchwegger, R., Pasche, B., Gerald, W., Dobles, M., Sorger, P.K., Murty, V.V., and Benezra, R. (2001). MAD2 haplo-insufficiency causes premature anaphase and chromosome instability in mammalian cells. Nature *409*, 355–359.
14. Perera, D., Tilston, V., Hopwood, J.A., Barchi, M., Boot-Handford, R.P., and Taylor, S.S. (2007). Bub1 maintains centromeric cohesion by activation of the spindle checkpoint. Dev. Cell *13*, 566–579.
15. Rieder, C.L., Schultz, A., Cole, R., and Sluder, G. (1994). Anaphase onset in vertebrate somatic cells is controlled by a checkpoint that monitors sister kinetochore attachment to the spindle. J. Cell Biol. *127*, 1301–1310.
16. Petronczki, M., Siomos, M.F., and Nasmyth, K. (2003). Un menage a quatre: the molecular biology of chromosome segregation in meiosis. Cell *112*, 423–440.
17. Hunt, P., LeMaire, R., Embury, P., Sheean, L., and Mroz, K. (1995). Analysis of chromosome behavior in intact mammalian oocytes: monitoring the segregation of a univalent chromosome during female meiosis. Hum. Mol. Genet. *4*, 2007–2012.
18. LeMaire-Adkins, R., Radke, K., and Hunt, P.A. (1997). Lack of checkpoint control at the metaphase/anaphase transition: a mechanism of meiotic nondisjunction in mammalian females. J. Cell Biol. *139*, 1611–1619.
19. Brunet, S., Pahlavan, G., Taylor, S., and Maro, B. (2003). Functionality of the spindle checkpoint during the first meiotic division of mammalian oocytes. Reproduction *126*, 443–450.
20. Wassmann, K., Niault, T., and Maro, B. (2003). Metaphase I arrest upon activation of the Mad2-dependent spindle checkpoint in mouse oocytes. Curr. Biol. *13*, 1596–1608.
21. Homer, H.A., McDougall, A., Levasseur, M., Murdoch, A.P., and Herbert, M. (2005). Mad2 is required for inhibiting securin and cyclin B degradation following spindle depolymerisation in meiosis I mouse oocytes. Reproduction *130*, 829–843.
22. Homer, H.A., McDougall, A., Levasseur, M., Yallop, K., Murdoch, A.P., and Herbert, M. (2005). Mad2 prevents aneuploidy and premature proteolysis of cyclin B and securin during meiosis I in mouse oocytes. Genes Dev. *19*, 202–207.
23. Kudo, N.R., Wassmann, K., Anger, M., Schuh, M., Wirth, K.G., Xu, H., Helmhart, W., Kudo, H., Mckay, M., Maro, B., et al. (2006). Resolution of chiasmata in oocytes requires separase-mediated proteolysis. Cell *126*, 135–146.

24. Tsurumi, C., Hoffmann, S., Geley, S., Graeser, R., and Polanski, Z. (2004). The spindle assembly checkpoint is not essential for CSF arrest of mouse oocytes. J. Cell Biol. *167*, 1037–1050.
25. Niault, T., Hached, K., Sotillo, R., Sorger, P.K., Maro, B., Benezra, R., and Wassmann, K. (2007). Changing Mad2 levels affects chromosome segregation and spindle assembly checkpoint control in female mouse meiosis I. PLoS ONE *2*, e1165.
26. Lewandoski, M., Wassarman, K.M., and Martin, G.R. (1997). Zp3-cre, a transgenic mouse line for the activation or inactivation of loxP-flanked target genes specifically in the female germ line. Curr. Biol. *7*, 148–151.
27. Epifano, O., Liang, L.F., Familari, M., Moos, M.C., Jr., and Dean, J. (1995). Coordinate expression of the three zona pellucida genes during mouse oogenesis. Development *121*, 1947–1956.
28. Ledan, E., Polanski, Z., Terret, M.E., and Maro, B. (2001). Meiotic maturation of the mouse oocyte requires an equilibrium between cyclin B synthesis and degradation. Dev. Biol. *232*, 400–413.
29. Reis, A., Chang, H.Y., Levasseur, M., and Jones, K.T. (2006). APCcdh1 activity in mouse oocytes prevents entry into the first meiotic division. Nat. Cell Biol. *8*, 539–540.
30. Clute, P., and Pines, J. (1999). Temporal and spatial control of cyclin B1 destruction in metaphase. Nat. Cell Biol. *1*, 82–87.
31. Hagting, A., Den Elzen, N., Vodermaier, H.C., Waizenegger, I.C., Peters, J.M., and Pines, J. (2002). Human securin proteolysis is controlled by the spindle checkpoint and reveals when the APC/C switches from activation by Cdc20 to Cdh1. J. Cell Biol. *157*, 1125–1137.
32. Herbert, M., Levasseur, M., Homer, H., Yallop, K., Murdoch, A., and McDougall, A. (2003). Homologue disjunction in mouse oocytes requires proteolysis of securin and cyclin B1. Nat. Cell Biol. *5*, 1023–1025.
33. Wu, J.Q., Hansen, D.V., Guo, Y., Wang, M.Z., Tang, W., Freel, C.D., Tung, J.J., Jackson, P.K., and Kornbluth, S. (2007). Control of Emi2 activity and stability through Mos-mediated recruitment of PP2A. Proc. Natl. Acad. Sci. USA *104*, 16564–16569.
34. Kueng, S., Hegemann, B., Peters, B.H., Lipp, J.J., Schleiffer, A., Mechtler, K., and Peters, J.M. (2006). Wapl controls the dynamic association of cohesin with chromatin. Cell *127*, 955–967.
35. Reis, A., Madgwick, S., Chang, H.Y., Nabti, I., Levasseur, M., and Jones, K.T. (2007). Prometaphase APCcdh1 activity prevents non-disjunction in mammalian oocytes. Nat. Cell Biol. *9*, 1192–1198.
36. Kouznetsova, A., Lister, L., Nordenskjold, M., Herbert, M., and Hoog, C. (2007). Bi-orientation of achiasmatic chromosomes in meiosis I oocytes contributes to aneuploidy in mice. Nat. Genet. *39*, 966–968.
37. Stegmeier, F., Rape, M., Draviam, V.M., Nalepa, G., Sowa, M.E., Ang, X.L., McDonald, E.R., 3rd, Li, M.Z., Hannon, G.J., Sorger, P.K., et al. (2007). Anaphase initiation is regulated by antagonistic ubiquitination and deubiquitination activities. Nature *446*, 876–881.
38. Reddy, S.K., Rape, M., Margansky, W.A., and Kirschner, M.W. (2007). Ubiquitination by the anaphase-promoting complex drives spindle checkpoint inactivation. Nature *446*, 921–925.
39. Palframan, W.J., Meehl, J.B., Jaspersen, S.L., Winey, M., and Murray, A.W. (2006). Anaphase inactivation of the spindle checkpoint. Science *313*, 680–684.
40. Kraft, C., Herzog, F., Gieffers, C., Mechtler, K., Hagting, A., Pines, J., and Peters, J.M. (2003). Mitotic regulation of the human anaphase-promoting complex by phosphorylation. EMBO J. *22*, 6598–6609.
41. Herzog, F., Mechtler, K., and Peters, J.M. (2005). Identification of cell cycle-dependent phosphorylation sites on the anaphase-promoting complex/cyclosome by mass spectrometry. Methods Enzymol. *398*, 231–245.
42. Holt, L.J., Krutchinsky, A.N., and Morgan, D.O. (2008). Positive feedback sharpens the anaphase switch. Nature *454*, 353–357.
43. Reddy, P., Liu, L., Adhikari, D., Jagarlamudi, K., Rajareddy, S., Shen, Y., Du, C., Tang, W., Hamalainen, T., Peng, S.L., et al. (2008). Oocyte-specific deletion of Pten causes premature activation of the primordial follicle pool. Science *319*, 611–613.
44. Bernard, P., Maure, J.F., and Javerzat, J.P. (2001). Fission yeast Bub1 is essential in setting up the meiotic pattern of chromosome segregation. Nat. Cell Biol. *3*, 522–526.
45. Kitajima, T.S., Hauf, S., Ohsugi, M., Yamamoto, T., and Watanabe, Y. (2005). Human Bub1 defines the persistent cohesion site along the mitotic chromosome by affecting Shugoshin localization. Curr. Biol. *15*, 353–359.
46. Riedel, C.G., Katis, V.L., Katou, Y., Mori, S., Itoh, T., Helmhart, W., Galova, M., Petronczki, M., Gregan, J., Cetin, B., et al. (2006). Protein phosphatase 2A protects centromeric sister chromatid cohesion during meiosis I. Nature *441*, 53–61.
47. Wirth, K., Wutz, G., Kudo, N.R., Desdouets, C., Zetterberg, A., Taghybeeglu, S., Seznec, J., Ducos, G., Ricci, R., Firnberg, N., et al. (2006). Separase: a universal trigger for sister chromatid disjunction but not chromosome cycle progression. J. Cell Biol. *172*, 847–860.
48. Wirth, K.G., Ricci, R., Gimenez-Abian, J.F., Taghybeeglu, S., Kudo, N.R., Jochum, W., Vasseur-Cognet, M., and Nasmyth, K. (2004). Loss of the anaphase-promoting complex in quiescent cells causes unscheduled hepatocyte proliferation. Genes Dev. *18*, 88–98.
49. Hodges, C.A., and Hunt, P.A. (2002). Simultaneous analysis of chromosomes and chromosome-associated proteins in mammalian oocytes and embryos. Chromosoma *111*, 165–169.
50. Peters, A.H., Plug, A.W., van Vugt, M.J., and de Boer, P. (1997). A drying-down technique for the spreading of mammalian meiocytes from the male and female germline. Chromosome Res. *5*, 66–68.
51. Rabut, G., and Ellenberg, J. (2004). Automatic real-time three-dimensional cell tracking by fluorescence microscopy. J. Microsc. *216*, 131–137.